Cone-Beam CT Artefact Reduction, Using Efficient Transfer Learning

Placeholder for final title

Eindhoven Institute of Technology

Medical Image Analysis Group
Florian Delberghe

Eindhoven, TU/e, 2020

Contents

1 Introduction

Lorem ipsum dolor sit amet, consectetuer adipiscing elit. Ut purus elit, vestibulum ut, placerat ac, adipiscing vitae, felis. Curabitur dictum gravida mauris. Nam arcu libero, nonummy eget, consectetuer id, vulputate a, magna. Donec vehicula augue eu neque. Pellentesque habitant morbi tristique senectus et netus et malesuada fames ac turpis egestas. Mauris ut leo. Cras viverra metus rhoncus sem. Nulla et lectus vestibulum urna fringilla ultrices. Phasellus eu tellus sit amet tortor gravida placerat. Integer sapien est, iaculis in, pretium quis, viverra ac, nunc. Praesent eget sem vel leo ultrices bibendum. Aenean faucibus. Morbi dolor nulla, malesuada eu, pulvinar at, mollis ac, nulla. Curabitur auctor semper nulla. Donec varius orci eget risus. Duis nibh mi, congue eu, accumsan eleifend, sagittis quis, diam. Duis eget orci sit amet orci dignissim rutrum.

Nam dui ligula, fringilla a, euismod sodales, sollicitudin vel, wisi. Morbi auctor lorem non justo. Nam lacus libero, pretium at, lobortis vitae, ultricies et, tellus. Donec aliquet, tortor sed accumsan bibendum, erat ligula aliquet magna, vitae ornare odio metus a mi. Morbi ac orci et nisl hendrerit mollis. Suspendisse ut massa. Cras nec ante. Pellentesque a nulla. Cum sociis natoque penatibus et magnis dis parturient montes, nascetur ridiculus mus. Aliquam tincidunt urna. Nulla ullamcorper vestibulum turpis. Pellentesque cursus luctus mauris.

Nulla malesuada porttitor diam. Donec felis erat, congue non, volutpat at, tincidunt tristique, libero. Vivamus viverra fermentum felis. Donec nonummy pellentesque ante. Phasellus adipiscing semper elit. Proin fermentum massa ac quam. Sed diam turpis, molestie vitae, placerat a, molestie nec, leo. Maecenas lacinia. Nam ipsum ligula, eleifend at, accumsan nec, suscipit a, ipsum. Morbi blandit ligula feugiat magna. Nunc eleifend consequat lorem. Sed lacinia nulla vitae enim. Pellentesque tincidunt purus vel magna. Integer non enim. Praesent euismod nunc eu purus. Donec bibendum quam in tellus. Nullam cursus pulvinar lectus. Donec et mi. Nam vulputate metus eu enim. Vestibulum pellentesque felis eu massa.

2 Literature Review

Summary

2.1 Introduction

2.1.1 The Need and Uses for Tomography

Imaging has become an indispensable tool in the clinical field over the last decades. Its uses are mutli-fold, as a diagnostic tool it can be helpfull for early detection of pathologies and their monitoring over time. Once diagnostic has been established, imaging can be fundamental in planning surgery paths and guiding radiotherapies. Starting in the 1970s a new imaging modality arose, computed tomography, solving the lack of depth information in X-ray imaging and furthering the technique of tomosythesis. It has helped advance the field of medicine by providing clinicians with less invasive ways of seeing the insides of the human body. Few generations of computed tomography (CT) have come and went as the focus is put on higher resolution, faster acquisition times and dose reduction. The major issue of computed tomography that remains is the issue of large amounts of radiation exposure to the patients; especially for more routine surgeries where irradiation isn't worth its consequences or for follow up of subject that requires many imaging sessions. This is why CT has been phased out in favor of other modalities such as ultrasounds or MRI in recent years for many tasks. There althought remain some tasks for which CT imaging is unchallenged, such as imaging of bone structures, fast (sub-second) volume acquistion, etc.

One of the most recent CT imaging advances was the use of Cone-Beam X-ray sources for acquitition, this allows to acquire anywhere from multiple slices to a full volume in a single pass.

2.1.2 Computed Tomography, from 1st to 4/6th Generation

The inception of the Computed Tomography can be traced all the way back to X-ray imaging; it was one of the first ways to see insides of the human body without invasive and potentially dangerous (at the time) surgical procedures **[REF]**. The main issue with X-rays was their lack of depth information, as all of the morphological structures were projected on the imaging plane. Some expert knowledge in the field can be enough to counteract this limitation for some use cases but the need for better techniques were being felt.

The first generation of CT (Hounsfield (1973)), using slide-then-rotate mouvements to sample a whole slice were awfully slow and had low resolution, its uses were thus limited to imaging slices of cranium in immobilized patients (Ambrose (1973)). Then subsequent advances in both hardware, such as fan-beam, helical scanning with slip ring technology, muti-rows detectors (MDCT) **[REF]**; as well as software where new reconstruction methods can accomodate emerging geometries, lower doses and faster scanning allowed the technology to branch out to a multitude of other imaging modalities. Adding to that newer statistical based methods for the more challenging tasks, helped push CT to its current state where good constrast can be had in most tissues and scanning times as well as radiation doses aren't as prohibitive.

2.2 Cone-Beam CT, its Uses and Drawbacks

2.2.1 What is Cone-Beam CT

The latest, innovation and the one at the center of our focus is Cone-Beam CT (CBCT), it was approved for use around 1996 in Europe, (2001 in the US) and is one of the most recent development in the field of CT imaging. This technique furthers the idea of MDCT (Multi Detector row CT) where the X-ray fan beam is collimated less tightly in the z-direction which allows the illumination of multiple rows of the X-ray detectors. These advances take their origins in the development of flat panel detectors that can stack multiple rows of X-ray sensitive pixels thus imaging a larger field of view. Since the geometry of Cone-Beam CT is different (illuminating rays not parallel to all imaging planes), the filtered backprojection used until then isn't applicable anymore since the further we stray from the middle plane the less the algorithm's hypothesis are valid, which breaks down the reconstruction. A new method was developed for CBCT, the FDK reconstruction algorithm (Feldkamp et al. (1984)); which can reconstruct volumes with non parallel ray geometries.

CBCT has today become a very important imaging modality for some fields, mostly in implant dentistry, orthopedics and interventional radiology (Venkatesh and Venkatesh Elluru (2017)). Its use in those specific fields is thanks to its ability to scan a volume in a single pass which can be fast and only require a low amount of radiation exposure. Its lower cost [REF?] also allows CBCT imaging systems to be deployed in smaller stuctures for wider availability of diagnostics around the world and non-destructive material testing at smaller scales.

2.2.2 Reconstruction Methods

The main methods for CT image reconstruction are based on theory discovered by John Radon (Radon (1986)). Where given only the projections of a density function, one can reconstruct the original density exactly. The mathematical framework of Radon space projection and reconstruction is well understood and has since its inception been adapted to work with the fan-beam and helical geometries of the newer generation scanner setups [REF]. In practice, the inverse Radon transform is equivalent with filtered backprojection methods so this is what is used in practice since it is more easily set up as a computationaly feasible algorithm. Even though we can find some similarities between helical fan beam CT and CBCT, there is actually a major difference, that is lack of information in the z-direction. The fan-beam helical geometry samples every slice sufficiently regarding the Nyquist-Shannon exact reconstruction criterion, even though the beams aren't perfectly colinear at opposite angles. Also for helical scanning setups, each slice isn't exactly sampled twice but some inter-slice interpolation method gets close to it in theory.

The issues that arise with Cone-Beam CT is that another kind of data insufficiency criterion is not met: Tuy-Smith's DSC Tuy (1983). It can be formulated as *"For every plane that intersect the object to be imaged it intersects the source trajectory at least once"*. In the case of Cone-Beam imaging with a single orbit however, the X-ray cone is only collinear to the single midline plane. This data insufficiency is still the root cause of most of the limitaions of the CBCT imaging method today, however a mathematical theory that is the basis for the reconstruction of cone beam acquired data was discovered by Feldkamp, Davis and Kress (Feldkamp et al. (1984)). The so called FDK reconstruction algorithm is an extension of the backprojection method for cone-beam geometry, and it allows for the correct weighting of divergent beams. Regular methods used for traditional CT reconstruction such as Fourier based methods L.A. Shepp (1974), that make use of the Fourier slice / section theorem to make parallels between Radon space where the data is aquired and forward / inverse Fourier transform along lines in space (which can be computed efficiently by modern computational methods such as FFT) cannot be used directly for cone beam due to different geometry and null space in the sampled Radon space. Algebraic methods (ART) **[REF]**, that are also commonly used also suffer from issues with the different geometry of cone beams. Overall the majority of the CBCT acquisition trajectories are using a single circular orbit around the object of interest this method does not however fullfill the DSC criterion for a perfect reconstruction and are the source of artefacts during approximate reconstruction.

2.2.3 Artefacts and Related Issues

As was introduced in the previous section, the sampling of a volume with a cone-shaped X-ray beam does not meet Tuy-Smith's DSC when using simple orbit trajectories. This causes missing information lying in a double inverted cone section within the Radon space. The geometry of the scanning process does not allow to sample the data within a full sphere in Radon space as would be required for perfect reconstruction which in turn leads to the formation of artefacts when reconstruction of the volume is computed [REF]. The null space having an inverted conical shape, artefacts become larger and more prevalent as the scanning angle and the size of the null space increase. This can be intuitively explained by the fact that the further away we are from the midplane the further the projection strays from a traditional parallel-(fan)-beam CT. The main artefacts that arises in CBCT is the presence of large streaking and shading artefacts near high density objects. Those ray looking artefacts happen to be colinear with the incident scanning X-ray beam. The second issue is shape deformation (streching in the axial direction), this is especially visible on Defringe phantoms [REF] that exacerbate this behavior. This can be attributed to the FDK reconstruction method, indeed, using a similar method to the usual backprojection or filtered backprojection has limitations when using cone-beam scanning. During the scanning orbit, some parts of the images are not in the beam's field of view for some range of angles and thus during reconstruction they lack projections from other points of view to counteract the values of the backprojected rays from dense parts of the volume. Those bright and dark streaks are the main focus of most of the CBCT artefact reduction methods. Finnaly CBCT also suffers from its inherent lack of good soft tissue contrast [REF?] unlike its parallel beam counterpart, meaning that it is relegated to bone and teeth imaging tasks (or angiography with contrast injection [REF?])

2.3 Newer Methods for Reconstruction and Artifact Reduction

2.3.1 Two-Pass Reconstruction

One of the first method for artifact reduction in CBCT images was (Hsieh (2000)), it came from the observation that the majority of cone-beam artefacts appear over medium density objects from extremly high or low density objects, (extreme density or ED objects from now on) causing streaking and shading respectively. This is due to the way the FDK based backprojection algorithm cannot perfectly reconstruct slices outside of the mid-plane exactly (loss of validity of the Fourier slice theorem). Using the FDK reconstructed image as a starting point (first pass) they propose to segment out the ED objects with a simple thresholding method. From the extracted ED objects one can syntheticaly reconstruct the artefacts with simple forward projections at a lower resolution (into several classes if needed) they substract the original images from it thus creating noise-only images. Finnaly with some processing, image transfer functions to mimic the imaging modalities, one can created a final volume with a significant reduction in artifacts (second pass). While this is a good technique and requires minimal extra computational capacity it is also limited to small cone angles and high density bones. The clinical uses were at best limited, concept was furthered by (Han and Baek (2019)) and (Hsieh et al. (2000)).

2.3.2 Iterative Methods

The next step for CT reconstruction is the use of iterative methods, the need for such methods occurs in challenging situations when one pass, such as (filtered) backprojection, or two passes are not enough to sufficiently reconstruct a CT image or even if one desires better image quality in general at the expense of additional computation. Iterative methods were how the problem of CT reconstruction was initially solved **[REF]** but filtered backprojection was then selected as the main reconstruction modality for its speed of image reconstruction. Lately with the advances in computer hardware and the algorithms that could take advantage of GPUs (Jia et al. (2011)), it is becoming possible to use iterative methods commonly in a clinical settings. The main advantage of iterative methods is the ability to add some prior knowledge to the reconstruction, this can include modelling the noise or other peculiarities of the imaging system. The way it works is to make a first assumption about the attenuation density image (it can start with a back-projected image, an empty one as well as anything in between). From this, one computes the differences between the acquired projection data and projection of the reconstructed image at each iteration and refines the current guess so that it matches the acquired data better. Usually the system to solve is overdetermined since there is a lot more projections than voxels to reconstruct therefore some kind of normalization must be employed to prevent the problem from having singular matrices that can't be inverted.

$$arg\,\underset{x}{min} = \|Ax - p\| + reg(x)$$

Those regularization functions are usefull in making the optimisation landscape of the loss smoother and convex. Every step of the iterative method is usually performed with a gradient descent (or GD derived) method. The uses for iterative methods span a very wide area, from low-dose CT scans [REF] to compressed sensing (Choi et al. (2010)) going through cone-beam and motion artefact reduction [REF] and cross modal registration (Nithiananthan et al. (2011)). The most well known and used is probably the SART method (Simultaneous Algebraic Reconstruction Technique) [REF]. Today iterative methods are widly used in the clinical and experimental settings and some form of it is present in most CT scanners availble today from any seller.

- Mathmatical setup (Loss, max likelihood estimation, or MAP)
- TV and other regularizations (Sidky and Pan (2008))

2.3.3 Deep Learning Based Methods

Deep learning has been an ever more present way of solving problems in every field, due to their large learning capacities and high adaptability. It's historically main task of classifiacation can also be adapted to medical images and CBCT (Miki et al. (2017)). Similarly to classification where the models need to retain some information about the image statistics of certain regions to segment or classify them; we can see how similarly to the iterative methods, the use of deep learning based models can help provide a huge amount of prior information about the CT images (given enough and good enough training data), instead of relying on manually engineered features, information that can then be used to remove artefacts and noise efficiently. The deep learning models can be used for image domain translation from CBCT to CT and back using cycle-GANs and residual layers (Lei et al. (2019)). Also some proof of concept for intensity correction in CBCT to make it comparable with conventional volumetric CT (Hansen et al. (2018)). Most of the developements that are interesting to us are more in the task of artefact reduction and compressed sensing methods that usually happend to reduce reconstruction artefacts as a by product. Some of those techniques can be found looking for example at the top proposed methods of the grand low-dose CT challenge [REF?]. The most common architecture type that we can find is an iteration on some type of encoder-decoder model where the input data is projected onto a lower dimension manifold that is engineered to capture the data structure. After that the data is reconstructed to its required dimensionality given that in theory only the image structure is kept in the encoding bottleneck, the reconstructed images should have a reduced amount of noise and artifacts. An example of that is the with residual and skip connections is presented in (Chen et al. (2017)). Computed tomography isn't the only imaging modality where there is a need for artefact reduction and reconstruction from limited data sampling, compressed sending in MRI is a large area of research to which many deep learning models have been applied, (Yang et al. (2017)). More recently some lighter models take advantage of dense multi-scale convolution to produce promissing results in artefact reduction in CBCT (Huang et al. (2018), Pelt and Sethian (2018)).

The field of inverse problem solving remains vast and deep learning based methods are ever more plentyfull (Ongie et al. (2020))

2.4 Transfer Learning in Inverse Problems

2.4.1 Transfer Learning in Medical Imaging

The task of training deep learning models on medical images, is quite challenging, mainly regarding the lack of availability of data because of its sparseness for certain tasks and patient privacy concerns. Counterintuitively the datasets can also be too large, to fit in system momery or for dense prediction by classical models. On top of acquisition, labelling such data quickly becomes an expensive task since it requires domain experts. Those are the main reasons transfer learning is gaining in interest, indeed, it could help in reducing or eliminating some of those expensive and time consuming steps. **Give more exmaples!**

2.4.2 Transfer for Regression / Inverse Mapping Tasks

TODO

2.5 Conclusion

In conclusion new advances in medical imaging could greatly help reduce the major issues of patient exposure to ionizing radiation. However, being inherently limited by their geometry and the reconstruction methods their widespread use is not possible as of yet. As iterative methods have caught up to combat some of those limitations, they still remain bound to selected tasks since they need large amounts of computation to perform well and can not be used for high throughput tasks. Given that, faster methods using deep learning to inject prior knowledge into the denoising and reconstruction models are being heavily researched today thanks to their promissing abilities and faster / better performances. The main limitation preventing their widespread use are the difficulties in getting those methods approves due to their "black-box" nature and low interpretability. Training those models can quickly become the limiting factor in the context of medical imaging where the procurement of data isn't easy. Therefore, transfer learning seems to be the best technique to make the best out of the availble data and promising models. We will now research:
What is the quality and quantity of information needed to efficiently transfer knwoledge in deep learning based artifact reduction methods for cone-beam CT imaging?

3 Experiments Journal

3.1 Training on Phantoms & Walnuts

3.1.1 Scale in/out Parameter extimation

For the MSDNet model to train optimaly, the inputs and outputs are standardize ($\sim \mathcal{N}(0,1)$). Therefore we need to estimate a good estimate of the statistics of the input and target images. Sampling the whole distribution can be costly and quickly run into issues with diminishing returns. We sample increasingly larger fractions of the training datasets (Walnuts and Phantoms) and observe how quickly we converge to the true statistics. From Figure 3.1, it seems that a third of the dataset is good compromise between computation time and accuracy of the estimation.

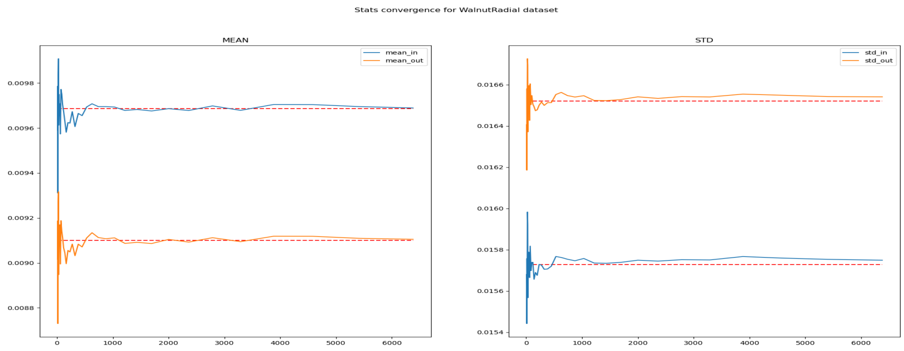

(a) Walnut Dataset

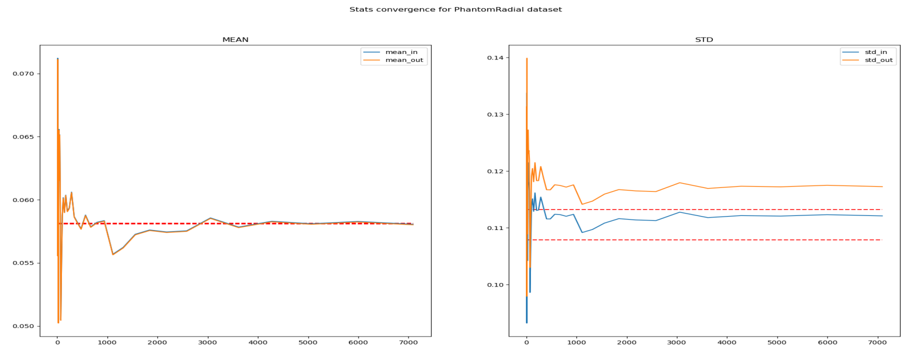

(b) Phantom Dataset

Figure 3.1: Dataset Statistics Estimated on Samples (x axis # samples)

3.1.2 Walnuts

Dataset specifications:

- Walnuts 1-9
- 709 Radial slices sampled in $\theta \in [0, \pi[$
- Using sample 6 as validation (Walnut7)

`MSD_d30_walnuts`: Training 30 layers MSDNet with FastWalnuts2 ([1-9] walnuts, Walnut7 as validation set)
`MSD_d80_walnuts`: Training 80 layers MSDNet with FastWalnuts2 ([1-9] walnuts, Walnut7 as validation set)
No regularisation, $lr = 2 \cdot 10^{-3}$, Figure 3.2 **[ADD MEAN TRAINING TIME]**

Figure 3.2, shows the training and validation losses for the first 500 batches (500*32 samples). Shape of the curves, and the end losses after it settles are similar enough that smaller models can be used safely to experiment while keeping the experiment times low. Table 3.1 shows

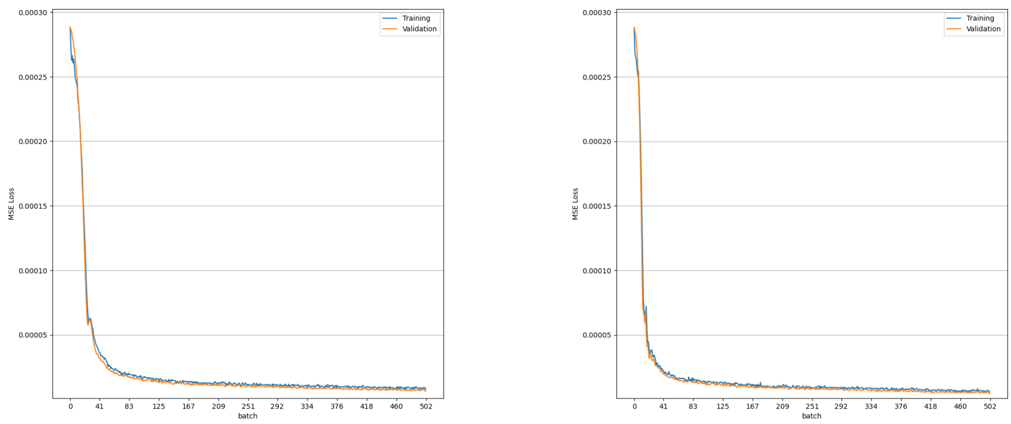

(a) 30 Layers MSDNet

(b) 80 Layers MSDNet

Figure 3.2: First Batches (32 samples) of Training for MSDNet with Walnut Dataset

Model d80		Mean	Std
	MSE	$2.34 \cdot 10^{-6}$	$\pm 6.47 \cdot 10^{-7}$
	SSIM	0.82	$\pm 3.32 \cdot 10^{-2}$
	DSC	0.98	$\pm 6.28 \cdot 10^{-3}$
Model d30		Mean	Std
	MSE	$3.06 \cdot 10^{-6}$	$\pm 6.50 \cdot 10^{-7}$
	SSIM	0.77	$\pm 3.87 \cdot 10^{-2}$
	DSC	0.97	$\pm 5.22 \cdot 10^{-3}$

Table 3.1: Performance of last models (after 20 epochs) on 100 samples of validation set

that the end MSE loss after 20 training epochs are of the same scale, same for the DSC results that are comparable in both. Only the SSIM changes significantly (-> look into why exactly).

3.1.3 Anthropomorphic Phantoms

Dataset specifications:

- Phantoms 1-10
- 709 Radial slices sampled in $\theta \in [0, \pi[$
- Using sample 6 as validation (Phantom7)

Dataset Preparation

Reconstruction of volumes from dataset: Imported images are scans from 5 different phantoms (in scans numbered 1-10 where phantom scan[mod 5]) The volumes can have different sizes: radial slices and scan volume are centered around the center to reconstruct 501^3 pixels volume. In Figure 3.3, the left are the target volumes (This is CBCT imaging but close enough to true since ray angle is small), on the right, the simulated CBCT images: notice the softer edges and "shadows" caused by the rays.

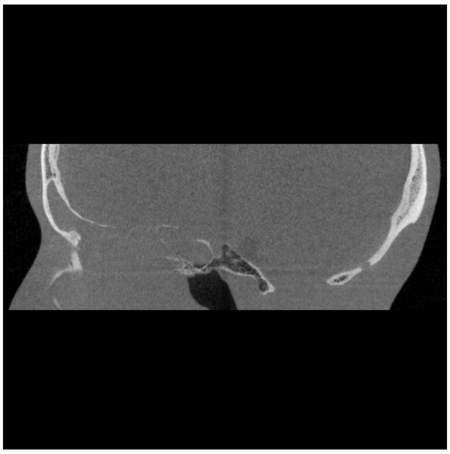

(a) "CT" Target Top of Volume

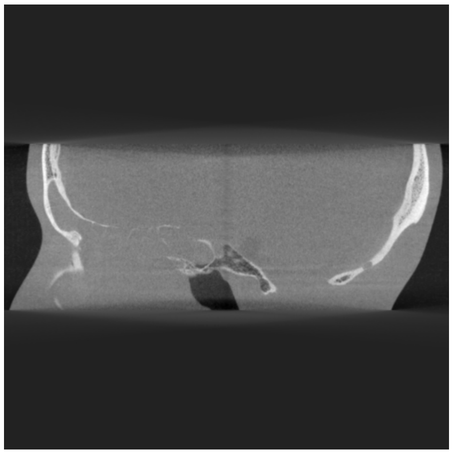

(b) CB Source Top of Volume

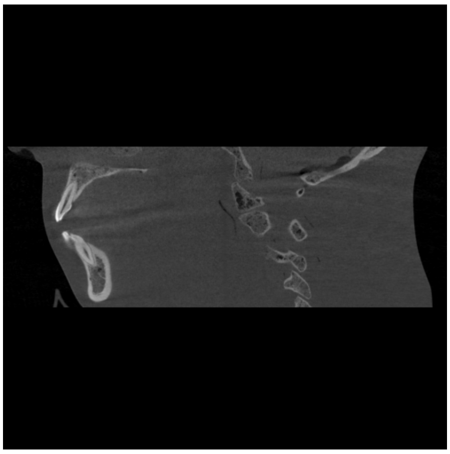

(c) "CT" Target Bottom of Volume

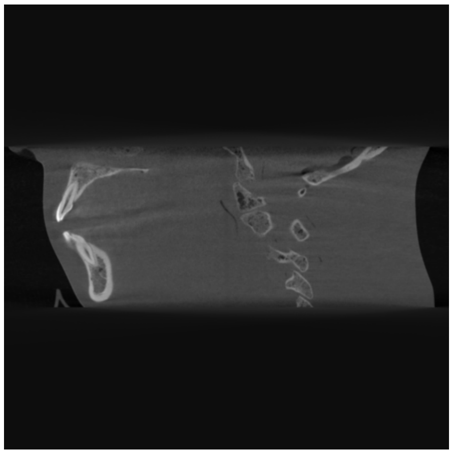

(d) CB Source Bottom of Volume

Figure 3.3: Anthropomorphic Phantom Dataset examples

3.1.4 Results of initial trainings

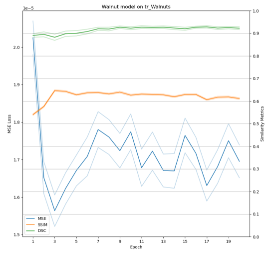

(a) Training Walnuts

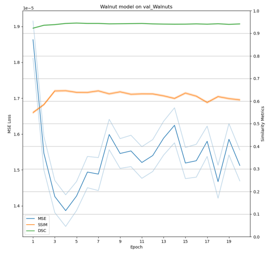

(b) Validation Walnuts

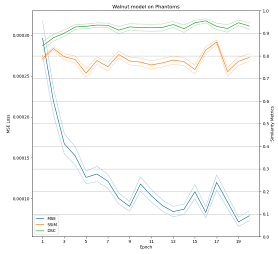

(c) Phantom Dataset

Figure 3.4: Walnut Trained Model Metrics on Different Datasets (200 Samples)

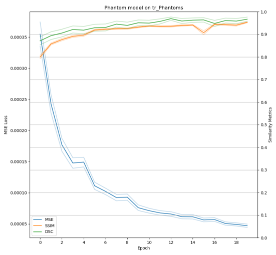

(a) Training Phantoms

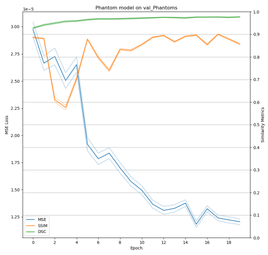

(b) Validation Phantoms

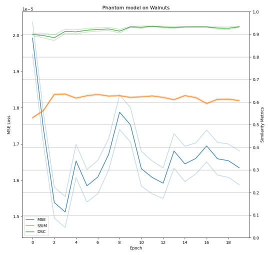

(c) Walnuts

Figure 3.5: Phantom (Scratch) Trained Model Metrics on Different Dataset (200 Samples)

3.1.5 Transfer Learning Experiments

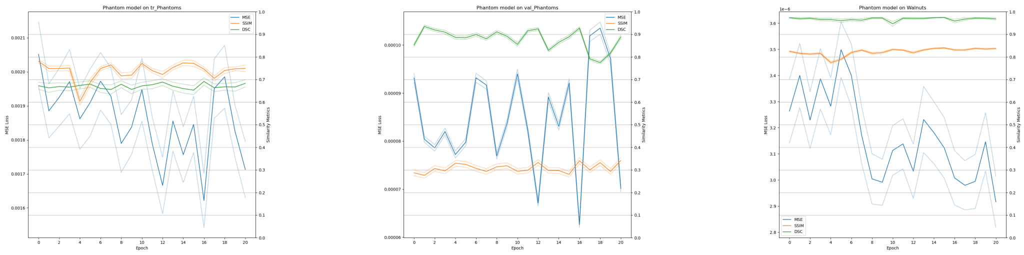

(a) Training Phantoms (b) Validation Phantoms (c) Walnut Dataset

Figure 3.6: Phantom (Transfer) Trained Model Metrics on Different Datasets (200 Samples)

Bibliography

Ambrose, J. (1973). Computerized transverse axial scanning (tomography): Part 2. Clinical application*. *The British Journal of Radiology*, 46(552):1023–1047.

Chen, H., Zhang, Y., Kalra, M. K., Lin, F., Chen, Y., Liao, P., Zhou, J., and Wang, G. (2017). Low-Dose CT with a Residual Encoder-Decoder Convolutional Neural Network (RED-CNN). *IEEE Transactions on Medical Imaging*, 36(12):2524–2535. arXiv: 1702.00288.

Choi, K., Wang, J., Zhu, L., Suh, T.-S., Boyd, S., and Xing, L. (2010). Compressed sensing based cone-beam computed tomography reconstruction with a first-order methoda): CBCT by compressed sensing. *Medical Physics*, 37(9):5113–5125.

Feldkamp, L. A., Davis, L. C., and Kress, J. W. (1984). Practical cone-beam algorithm. *Journal of the Optical Society of America A*, 1(6):612.

Han, C. and Baek, J. (2019). Multi-pass approach to reduce cone-beam artifacts in a circular orbit cone-beam CT system. *Optics Express*, 27(7):10108.

Hansen, D. C., Landry, G., Kamp, F., Li, M., Belka, C., Parodi, K., and Kurz, C. (2018). ScatterNet: A convolutional neural network for cone-beam CT intensity correction. *Medical Physics*, 45(11):4916–4926.

Hounsfield, G. N. (1973). Computerized transverse axial scanning (tomography): Part 1. Description of system. *The British Journal of Radiology*, 46(552):1016–1022.

Hsieh, J. (2000). Two-pass algorithm for cone-beam reconstruction. pages 533–540, San Diego, CA.

Hsieh, J., Molthen, R. C., Dawson, C. A., and Johnson, R. H. (2000). An iterative approach to the beam hardening correction in cone beam CT. *Medical Physics*, 27(1):23–29.

Huang, G., Chen, D., Li, T., Wu, F., van der Maaten, L., and Weinberger, K. Q. (2018). Multi-Scale Dense Networks for Resource Efficient Image Classification. *arXiv:1703.09844 [cs]*. arXiv: 1703.09844.

Jia, X., Dong, B., Lou, Y., and Jiang, S. B. (2011). GPU-based iterative cone-beam CT reconstruction using tight frame regularization. *Physics in Medicine and Biology*, 56(13):3787–3807.

L.A. Shepp (1974). The Fourier reconstruction of a head section. In *IEEE Transactions on Nuclear Science*, volume 21, page 21.

Lei, Y., Wang, T., Harms, J., Shafai-Erfani, G., Dong, X., Tang, X., Liu, T., Curran, W. J., Higgins, K., Zhou, J., Patel, P., and Yang, X. (2019). Image quality improvement in cone-beam CT using deep learning. In Bosmans, H., Chen, G.-H., and Gilat Schmidt, T., editors, *Medical Imaging 2019: Physics of Medical Imaging*, page 78, San Diego, United States. SPIE.

Miki, Y., Muramatsu, C., Hayashi, T., Zhou, X., Hara, T., Katsumata, A., and Fujita, H. (2017). Classification of teeth in cone-beam CT using deep convolutional neural network. *Computers in Biology and Medicine*, 80:24–29.

Nithiananthan, S., Schafer, S., Uneri, A., Mirota, D. J., Stayman, J. W., Zbijewski, W., Brock, K. K., Daly, M. J., Chan, H., Irish, J. C., and Siewerdsen, J. H. (2011). Demons deformable registration of CT and cone-beam CT using an iterative intensity matching approach: Iterative intensity matching for CT-CBCT registration. *Medical Physics*, 38(4):1785–1798.

Ongie, G., Jalal, A., Metzler, C. A., Baraniuk, R. G., Dimakis, A. G., and Willett, R. (2020). Deep Learning Techniques for Inverse Problems in Imaging. *arXiv:2005.06001 [cs, eess, stat]*. arXiv: 2005.06001.

Pelt, D. M. and Sethian, J. A. (2018). A mixed-scale dense convolutional neural network for image analysis. *Proceedings of the National Academy of Sciences*, 115(2):254–259.

Radon, J. (1986). On the determination of functions from their integral values along certain manifolds. *IEEE Transactions on Medical Imaging*, 5(4):170–176.

Sidky, E. Y. and Pan, X. (2008). Image reconstruction in circular cone-beam computed tomography by constrained, total-variation minimization. *Physics in Medicine and Biology*, 53(17):4777–4807.

Tuy, H. K. (1983). An Inversion Formula for Cone-Beam Reconstruction. *SIAM Journal on Applied Mathematics*, 43(3):546–552.

Venkatesh, E. and Venkatesh Elluru, S. (2017). CONE BEAM COMPUTED TOMOGRAPHY: BASICS AND APPLICATIONS IN DENTISTRY. *Journal of Istanbul University Faculty of Dentistry*, 51(0).

Yang, Y., Sun, J., Li, H., and Xu, Z. (2017). ADMM-Net: A Deep Learning Approach for Compressive Sensing MRI. *arXiv:1705.06869 [cs]*. arXiv: 1705.06869.